

## The Interpretation of the EPR Spectra of the Amorphous State of Group VIB Hydride Radicals by Means of the Gas-phase Data

Yashige KOTAKE, Mitsuo ONO, and Keiji KUWATA

Department of Chemistry, Faculty of Science, Osaka University, Toyonaka, Osaka

(Received December 17, 1970)

A new procedure for the interpretation of the amorphous EPR spectra of the group VIB hydride radicals, *i.e.*, OH, SH, SeH, and TeH, is proposed. The point of this method is to combine the observed hyperfine structure of these radicals in the gas phase and the calculation of the anisotropic hyperfine coupling constant. For this purpose, the Slater orbital and analytical Hartree-Fock orbitals were examined as unpaired electron orbitals by the comparative calculation of the hfs constants. The accuracy of this method was evaluated successfully by applying it to the OH radical. Moreover, in the case of the SH radical the newly-observed spectra in the amorphous state could be assigned to the SH radical.

The hyperfine (hf) interaction in diatomic hydride radicals is an important factor in clarifying the mechanism of the hf splitting of the proton. It also gives much information about the hf interaction in the hydride fragment of polyatomic radicals. The C-H fragment in organic radicals has been the subject of many theoretical and experimental works,<sup>1)</sup> while the others have scarcely been investigated at all.

The EPR study of radicals trapped in a single crystal has given the most definite information about the hf interaction but simple radicals such as diatomic hydrides present experimental difficulties in the single crystal study, for they are too small to be stabilized easily; moreover, sometimes the presence of more than one orientation of radicals in the mother crystal makes the analysis difficult, as may be illustrated in the study of the hydroxy radical.<sup>2)</sup> Moreover, as far as these solid phase data are concerned, they are under the influence of a matrix effect of a crystalline field.

About Group VIB hydride radicals, *i.e.*, OH, SH, SeH, and TeH, though solid-phase EPR data are poor except for the OH radical, their electric dipole transitions have been observed in the gaseous flow system.<sup>3-7)</sup> The hyperfine structure (hfs) of the gas-phase spectra gives information about both the isotropic and anisotropic terms.

In this study we will propose a new procedure to evaluate the principal values of the hf-tensor by the analysis of the hfs of the gas-phase spectra with the aid of the theoretical calculation. The point of this method is to utilize the calculation of dipolar terms and to evaluate indirectly the Fermi contact term.

The usefulness of the method was confirmed for the OH radical, which has been intensively studied in the solid phase.

Moreover, the application to the SH radical gave a correct identification of the radical trapped in the solid phase. The complex spectra obtained by Gunning *et al.*<sup>8)</sup> for SH were disproved by this application

and on the basis of the consideration of the *g*-tensor. The hf parameters estimated by this method fit well to those of the newly-observed spectra. On the SeH and TeH radicals, some information about hfs could be obtained.

In the calculation of the anisotropic terms, the characteristics of the Slater orbital and the analytical Hartree-Fock SCF atomic orbital of the Group VIB atom were also discussed.

### Theoretical

Because of the large rotational constants of Group VIB hydrides, they are not pure Hund's case (a) or (b) molecules. An intermediate coupling case between Hund's cases, (a) and (b), is treated in terms of Hund's (a) case. A small mixing of Hund's (b) case to a  $^2\Pi$  molecule can be expressed as a  $^2\Pi$  level slightly perturbed by a  $^2\Sigma$  level. The wavefunction is written as a linear combination of two  $^2\Pi$ 's and a  $^2\Sigma$  and the expansion coefficients are determined by the variation method using Van Vleck's matrix elements.<sup>9)</sup> In the case of Group VIB hydrides (ground state  $^2\Pi_{3/2}$ ,  $J=3/2$  in the case (a)), this wavefunction gives first-order expectation values,  $W_{\text{hfs}}^+$  and  $W_{\text{hfs}}^-$ , or Frosh-Foley's strong field hf hamiltonian<sup>10)</sup> for each of the lambda-doublets as follows:<sup>11)</sup>

$$W_{\text{hfs}}^+ = (A_1 + A_2)M_J M_I, \quad (1)$$

$$W_{\text{hfs}}^- = (A_1 - A_2)M_J M_I, \quad (2)$$

$$A_1 = [2a(2X + 2 - \lambda) + b(X + 16 - 2\lambda) + c(X + 4 - 2\lambda)]/15X, \quad (3)$$

$$A_2 = 2d(X - 2 + \lambda)/15X, \quad (4)$$

where:

$$X = [16 - \lambda(\lambda - 4)]^{1/2}, \quad (5)$$

Here  $\lambda$  is the ratio of the LS coupling constant to the rotational constant

and:

$$a = 2g_I\beta\beta_N\langle 1/r^3 \rangle_{\text{av}}, \quad (6)$$

$$b = -g_I\beta\beta_N\langle (3\cos^2\theta - 1)/r^3 \rangle_{\text{av}} + \frac{16\pi}{3}g_I\beta\beta_N\Psi^2(0), \quad (7)$$

9) J. H. Van Vleck, *Phys. Rev.*, **33**, 467 (1929).

10) R. A. Frosh and H. M. Foley, *ibid.*, **88**, 1337 (1952).

11) Eqs. (12a) and (12b) of Ref. 3.

1) For example, H. M. McConnell and D. B. Chesnut, *J. Chem. Phys.*, **27**, 984 (1957).

2) T. E. Gunter, *ibid.*, **46**, 3818 (1967).

3) H. E. Radford, *Phys. Rev.*, **122**, 114 (1961).

4) H. E. Radford, *ibid.*, **126**, 1035 (1962).

5) C. C. McDonald, *J. Chem. Phys.*, **39**, 2587 (1963).

6) H. E. Radford and M. Linzer, *Phys. Rev. Lett.*, **10**, 443 (1968).

7) H. E. Radford, *J. Chem. Phys.*, **40**, 2732 (1964).

8) D. A. Stiles, W. J. R. Tyerman, O. P. Strausz, and H. E. Gunning, *Can. J. Chem.*, **44**, 2149 (1966).

$$c = 3g_1\beta\beta_N\langle(3\cos^2\theta - 1)/r^3\rangle_{av}, \quad (8)$$

$$d = 3g_1\beta\beta_N\langle\sin^2\theta/r^3\rangle_{av}. \quad (9)$$

The coordinate used in these equations is shown in Fig. 1. These equations successfully explain the hfs of the OH<sup>3,4)</sup> and NO<sup>12)</sup> radicals.

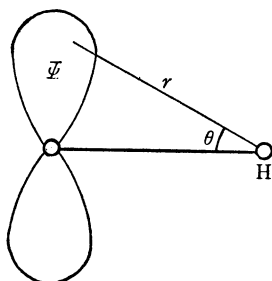


Fig. 1. Coordinate for Eqs. (6)–(9).

In Eq. (3) if  $a$ , the first term of  $b$  and  $c$ , can be calculated with sufficient accuracy, the Fermi contact term can be derived by putting the experimental values into  $A_1$  and  $X$ .

The molecular integrals such as  $\langle(3\cos^2\theta - 1)/r^3\rangle_{av}$  or  $\langle 1/r^3 \rangle_{av}$  can be calculated if an unpaired electron orbital and the interatomic distance are determined. If we adopt the LCAO-MO approximation in those hydrides, the unpaired electron orbital will be the  $np_x$  or  $np_y$  atomic orbital of the Group VIB atom, both orbitals are perpendicular to the molecular axis ( $z$ -axis). These atomic orbitals are frequently Slater orbitals or analytical Hartree-Fock (AHF) orbitals, the latter of which consist of a linear combination of Slater-type orbitals (STO).

An assumption of STO as an unpaired electron orbital made it possible to calculate these integrals analytically by the method of Barnett-Coulson.<sup>13)</sup> The method of McConnell and Strathdee<sup>14)</sup> is also applicable to the OH radical. Except for the STO of oxygen, however, it is, in fact, impossible to integrate analytically. For example, in the case of SeH, when we adopt the AHF orbital of selenium, 45 integrals must be calculated. Therefore, they are numerically integrated using Barnett-Coulson's formulation by means of an NEAC 2200—500 electronic computer. The upper limit of the numerical integration by Simpson's law was chosen so as to be five times larger than the equilibrium interatomic distance, for the contribution from the integration beyond this limit was smaller than five decimal places in the atomic unit.

From the Fermi contact term and the dipolar term, the principal values of the hf tensor,  $A_x$ ,  $A_y$ , and  $A_z$ , can be determined on the basis of the following assumption of axial symmetry:

$$A_x = A_y = b, \quad (10)$$

$$A_z = b + c. \quad (11)$$

These principal values are, however, essentially those for the free molecule; thus, there should be a

kind of limit in the comparison of the gas-phase hfs with the solid-phase one.

The dipolar term and other anisotropic terms reflect sharply the shape of the unpaired electron orbital of the radical; the calculation of their change with the interatomic distance is useful in examining this orbital. For example, the deviation of the value calculated by the Slater atomic orbital from the Hartree-Fock value will be a measure of its accuracy.

## Experimental

The method of observing gas-phase EPR spectra has been developed by Carrington and his colleagues.<sup>15)</sup> They designed new types of EPR cavities and pillboxes and observed several kind of new radicals. Among these radicals, the observation of OH, SH, and SeH is comparatively easy. The OH radical is produced by the microwave discharge of water, while the SH and the SeH radicals are produced by the reaction of the hydrogen atom with sulfur and selenium respectively. These spectra are electric dipole transitions between the lambda-type doublet, so the microwave must have an electrical component perpendicular to the external field. To create this condition, a TE<sub>012</sub> cylindrical cavity with a quartz pillbox was used. A rapid-gas-flow system consists of a ULVAC-300 rotary pump which evacuates 300 l per min, a liquid nitrogen trap 60 mm in diameter, a pilani-gauge, and an accurate needle valve. The linear velocity of the gas flow was supposed to be *ca.* 10 m/sec.

In a preliminary experiment, the gas-phase EPR spectra of OH, SH, and SeH were obtained with sufficient intensities. As for the TeH radical, the spectrum could not be obtained with a good SN ratio. The spectrometer used was operated in the X band with 455 kHz-field modulation and a 30 cm JEOL electromagnet.

In order to observe the solid-phase spectrum of the hydrides, under the same conditions as were used in the gas-phase experiment, the reactants were trapped at the point of the cavity in the gas-phase experiment on a coldfinger which was cooled at the temperature of liquid nitrogen. The outline of this apparatus is shown in Fig. 2. Except

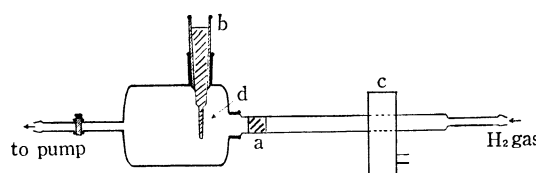


Fig. 2. Apparatus for trapping the radical in gas phase: a; evaporated film of S, Se, and Te, b; liq. N<sub>2</sub> Dewar vessel, c; cavity for discharge, d; coldfinger.

for OH, evaporated films of sulfur, selenium, and tellurium were made at the point of (a) in Fig. 2 and were attacked by the hydrogen atom which was generated in the microwave discharge of hydrogen gas. The microwave excitor was operated at 2450 MHz with a rectangular discharge cavity; its maximum output was 250 watt. The distance between the discharge (c) and the coldfinger (d) (*cf.* Fig. 2) was adjusted to get the best yield. The EPR measurement was done by transferring the coldfinger into a liquid-nitrogen Dewar vessel.

12) R. L. Brown and H. E. Radford, *Phys. Rev.*, **147**, 6 (1966).

13) M. P. Barnett and C. A. Coulson, *Phil. Trans. Roy. Soc.*, **243**, 221 (1951).

14) H. M. McConnell and J. Strathdee, *Mol. Phys.*, **2**, 129 (1959),

15) For example, A. Carrington, and D. H. Levy, *J. Phys. Chem.*, **71**, 2 (1967),

To identify the solid-phase spectra, dihydrides and dideuterides of sulfur, selenium, and tellurium which had been diluted in  $\text{H}_2\text{O}$  and  $\text{D}_2\text{O}$  matrices were irradiated by a UV light of a 1-kW high-pressure mercury arc at 77°K; the EPR spectra were also observed at the same temperature.  $\text{H}_2\text{Se}$  and  $\text{H}_2\text{Te}$  were formed by the hydrolysis of  $\text{Al}_2\text{Se}_3$  and  $\text{Al}_2\text{Te}_3$  respectively; the latter substances were synthesized by the ignition of Se and Te with Al.

### Results and Discussion

The lambda-type doubling frequencies,  $g$  values,  $A_1$  and  $A_2$  of OH, SH, SeH, and TeH and of their deuterides are tabulated in Table 1. The tendencies of the  $g$  value and the lambda-type doubling frequency, plus the molecular structure, can easily be explained by the theoretical expression of these constants.<sup>16)</sup>

In Table 2 the experimental values and the calculated values of hfs constants are listed.

**OH Radical.** As for the former data of the hfs constants determined by Radford,<sup>4)</sup> each experimental value could be compared to the calculated one. As can be seen in Table 2, the best accordance was obtained when the Slater orbital was adopted as an unpaired electron orbital. It may be noted that the unpaired electron orbital in the OH radical deviates from the pure  $2p$  orbital of oxygen upon the repulsion of the O-H bond and by the spin polarization of the inner shell. The Slater orbital, although it is a simple AO, may be supposed accidentally to include these effects.

In the MO calculation, the molecular integrals, such as overlap and Coulomb integrals, have been cal-

TABLE 1.  $g$ -FACTORS, LAMBDA-TYPE DOUBLING, AND hfs OF GROUP VIB HYDRIDE RADICALS ( $J=3/2$ )

	$g$ $((g_J^+ + g_J^-)/2)^a$	Lambda type doubling (MHz)	hfs constant		Ref.
			$A_1$ (MHz)	$A_2$ (MHz)	
OH	0.9556	1666.3	27.1	0.5	3
OD	0.8895	310.1	4.8	—	3
SH	0.8379	111.4	5.6	—	6
SD	0.8344	34.3	1.0	—	this work
SeH	0.8080	14.4	1.9	—	7
SeD	0.8061	1.9	—	—	17
TeH	0.8037	6.6	1.8	—	7

a)  $g_J^+$  and  $g_J^-$  denote the observed  $g$ -factors of each lambda type doublet.

TABLE 2. Hfs CONSTANTS OF GROUP VIB HYDRIDE RADICALS

		$2g_I\beta\beta_N\langle 1/r^3 \rangle_{av.}$ (MHz)	$g_I\beta\beta_N\langle (3\cos^2\theta - 1)/r^3 \rangle_{av.}$ (MHz)	$16/3\pi g_I\beta\beta_N\Psi^2(0)$ (MHz)	Parameters used for calculation
OH	Obsd {gas	86.0	44.4	-74.8	$R_e$ : UV <sup>d)</sup> $\lambda$ : Microwave <sup>e)</sup>
	solid	—	—	-75	
	Calcd (Slater)	84.0	46.0	-73.4	
	Calcd (AHF) <sup>a)</sup>	80.1	40.8	-62.2	
SH	Calcd (Slater)	29.9	10.9	-23.2	$R_e$ : UV <sup>f)</sup> $\lambda$ : UV <sup>f)</sup>
	Calcd (AHF) <sup>b)</sup>	24.2	3.9	-5.9	
SeH	Calcd $n=3.5$ (Slater)	24.3	9.2	-64.2	$R_e$ : EPR <sup>g)</sup> $\lambda$ : EPR <sup>g)</sup>
	$n=4.0$	42.9	7.3	-102.6	
	Calcd (AHF) <sup>c)</sup>	38.3	19.0	-114.9	
TeH	Calcd (Slater)	29.1	12.4	-98.1	$R_e$ : EPR <sup>h)</sup> $\lambda$ : EPR <sup>h)</sup>

a) E. Clementi, C. C. J. Roothaan, and M. Yoshimine, *Phys. Rev.*, **127**, 1618 (1962).

b) R. E. Watson and A. J. Freeman, *ibid.*, **123**, 521 (1961).

c) E. Clementi, *J. Chem. Phys.*, **41**, 303 (1962).

d) G. Herzberg, "Molecular Spectra and Molecular Structure I. Spectra of Diatomic Molecules," D. Van Nostrand, New York, N. Y. (1950), p. 560.

e) Ref. 16.

f) D. A. Ramsay, *J. Chem. Phys.*, **20**, 1920 (1952).

g) Ref. 17.

h) Ref. 7.

16) G. C. Dousmanis, T. M. Sanders, Jr., and C. H. Townes, *Phys. Rev.*, **100**, 1735 (1955).

17) A. Carrington, G. N. Currie, and N. J. D. Lucas, *Proc. Roy. Soc.*, **A315**, 355 (1970).

culated by using the Slater orbitals. These integrals in the long internuclear distance differ from the AHF values. This property of the Slater orbital in the longer range appears less strongly for the dipolar term, which depends on  $r^{-3}$ , because it sharply decreases with  $r$ . As is well known,  $\langle 1/r^3 \rangle_{av}$  is a constant which shows the interaction between the hydrogen nucleus and the magnetic field generated by the orbital motion of an unpaired electron in a  $p$  orbital, so the inner shell spin density, which is induced by the spin polarization, has no effect on this constant. On the other hand, as the other anisotropic terms are originated by the interactions between the magnetic dipole of an unpaired electron and a hydrogen nucleus, the unpaired electron density in  $s$  orbital also has a small value. When a pure  $2p$  atomic orbital is adopted as the unpaired electron orbital it is reliably established that the calculated value of the anisotropic terms except  $\langle 1/r^3 \rangle_{av}$  deviate a little from the experimental value.

Concerning the Fermi contact term, the good agreement of the experimental value with the estimated one in anisotropic terms results in a good correspondence between the experimental and estimated values. The MO calculation of this term was done by Kayama.<sup>18)</sup> Introducing ten excited configurations to Freeman's LCAO-SCF-MO, he derived the value of  $-67.9$  MHz. It was a very good agreement considering the accuracy of ordinary MO calculations. According to his result, the absolute value of the Fermi contact term increases with the interatomic distance; at 2.2 a.u., it gives  $-99.4$  MHz. Even if we recognize the lack of monotony of the dependence of the  $\sigma$ - $\pi$  interaction on the interatomic distance, however, his value at 2.2 a.u. is too large.<sup>19)</sup>

The principal values of the hf-tensor of the OH radical, as determined by several investigators and as calculated by the method explained in the theoretical section, are listed in Table 3. Though the values obtained from the analysis of the solid-phase EPR spectra of the OH radical did not agree very well, the calculated results agreed fairly well.

By considering the accuracy of the above calculation of the anisotropic terms, the method of deriving the principal values of the hf-tensor can be said to be applicable when the appropriate atomic orbital for the unpaired electron orbital can be found.

18) K. Kayama, *J. Chem. Phys.*, **39**, 1507 (1963).

19) We calculated the Fermi term of OH by Pople's INDO (Intermediate Neglect of Differential Overlap) method. By the approximate estimation of the one-center exchange integral of the oxygen and other integrals calculated from Pople's proposal, the SCF process repeated about forty times gave the final spin density as  $\rho_{2p_x,y}=1.000$  or 0,  $\rho_{3p_z}=0.094$ ,  $\rho_{2s}=-0.065$ , and  $\rho_{1sH}=-0.029=-41.3$  MHz. Moreover, the dependence of the spin density of the H atom on the interatomic distance was:

	1.8342 a.u.	2.0 a.u.	2.2 a.u.
SCF-CI	-0.048	-0.056	-0.070
INDO	-0.029	-0.021	-0.013

At the equilibrium distance, the error of the value was bigger than Kayama's result, but the absolute value decreases with an increase in the interatomic distance.

TABLE 3. HF-TENSOR OF OH RADICAL

	$A_x$ (gauss)	$A_y$	$A_z$	Ref.
Calcd				
Slater	-42.6	-42.6	6.4	
AHF	-36.7	-36.7	6.9	
Obsd				
gas	-42.6	-42.6	5.0	4
ice	$-26 \pm 4$	$-44 \pm 2$	$0 \pm 6$	a
ice	$-26 \pm 3$	$-43.7 \pm 0.05$	$\pm 5 \pm 5$	b
CaSO <sub>4</sub> ·2H <sub>2</sub> O	-32.5	-43	3.3	2

a) J. A. Brivati, M. C. R. Symons, D. J. A. Tinling, H. W. Wardale, and D. O. Williams, *Chem. Commun.*, **1965**, 402.

c) G. H. Dibdin, *Trans. Faraday Soc.*, **63**, 2098 (1967).

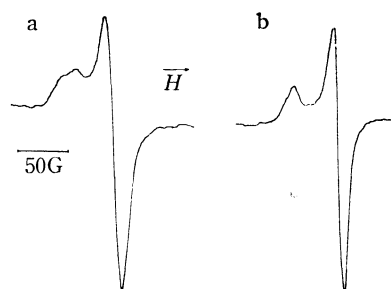


Fig. 3. EPR spectra of discharged product of a, H<sub>2</sub>O and b, D<sub>2</sub>O.

Figure 3 shows the EPR spectrum of the radical which is generated by the gas-phase microwave discharge of water and trapped at the temperature of liquid nitrogen. This spectrum shows no characteristic doublet of the OH radical, which was observed by the  $\gamma$ -ray<sup>20)</sup> or tritium  $\beta$ -ray<sup>21)</sup> irradiation of polycrystalline ice; it coincides with that from UV-irradiated H<sub>2</sub>O<sub>2</sub> of a 20% aqueous solution.

From deuterium substitution, this spectrum is found to consist of two radical species; by a detailed analysis of the far-ultra violet photolysis of water and other related compounds these two species were identified as the HO<sub>2</sub> and HO<sub>3</sub> radicals.<sup>22)</sup> The OH radical, which gives a strong EPR spectrum in the gas-phase, could not be observed in the trapped phase. This phenomenon corresponds to the fact that the UV photolysis of the dilute solution of hydrogen peroxide (less than 3 wt%) gives the OH radical, while a more concentrated solution never gives it. This proves that, in the solid phase, the OH radicals may recombine easily; those in the gas-phase convert into HO<sub>2</sub> or other radicals as soon as they are trapped in the solid phase.

**SH Radical.** At the equilibrium interatomic distance, the calculated values from the Slater and AHF orbitals are rather different from each other. About the  $3p$  orbital, though the true atomic orbital has three nodal planes, the Slater  $p$  AO's are always

20) For example, P. N. Moorthy, and J. J. Weiss, *Phil. Mag.*, **10**, 659 (1964).

21) J. Kroh, B. C. Green, and J. W. T. Spinks, *J. Amer. Chem. Soc.*, **83**, 2201 (1961).

22) K. Kuwata, Y. Kotake, K. Inada, and M. Ono, to be published.

nodeless except for the origin, and generally the  $p$  Slater orbitals of different shell are nonorthogonal. The AHF atomic orbital for  $3p$  of sulfur has two nodes other than the origin and is orthogonal to the  $p$  orbitals of the other shell. As anisotropic terms depend strongly on the shape of the orbitals, these properties of the Slater orbital are fatal in calculating the integrals.

For these reasons even if the influence of S-H bonding is considered, the AHF atomic orbital is much more reliable than the Slater one as an unpaired electron orbital. Sometimes the  $d$  orbital of a sulfur atom contributes to the sulfur and other atom bonding, but in the case of SH, the *ab initio* calculation of the electronic structure by Cade and Huo<sup>23)</sup> showed that the contribution of the sulfur  $d$ -type orbital to the unpaired orbital is extremely small.

According to the hfs constants from the AHF wavefunction, the anisotropic term is much smaller than that of the OH radical; the estimated Fermi contact term also has a small negative value. The negative value of the Fermi term suggests that the mechanism of generating the isotropic hf interaction is the exchange interaction between the  $3p_x$  or  $3p_y$  orbital of a sulfur atom with the  $\sigma$  bond of SH.

The EPR spectra of the reactants under the same conditions as in the gas-phase experiment of SH are shown in Fig. 4. These spectra consist of the superposition of three peaks which show a deuterium substitution effect and the one broad singlet line. The

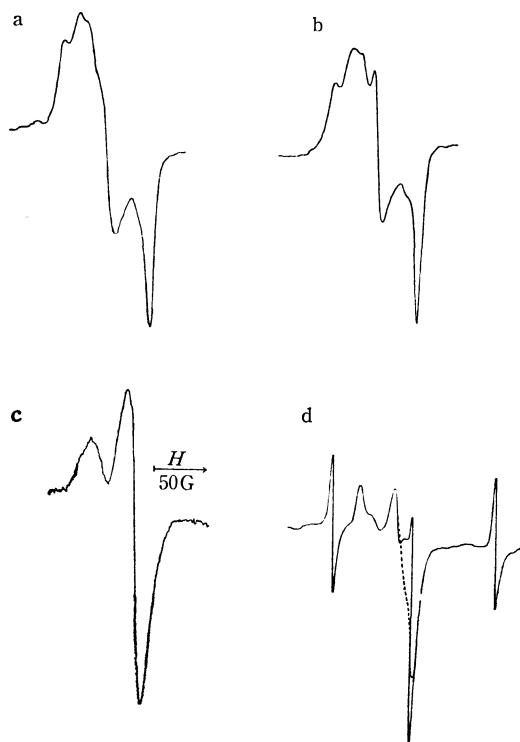


Fig. 4. EPR spectra of radicals formed by the reaction of sulfur with H atom (a), and D atom (b), and of UV photolyzed product of  $\text{H}_2\text{S}-\text{H}_2\text{O}$  system (c), and  $\text{D}_2\text{S}-\text{D}_2\text{O}$  system (d), broken line shows the subtraction of D atom spectrum from central part.

UV photolysis of the dilute solution of  $\text{H}_2\text{S}$  and  $\text{D}_2\text{S}$  gives a spectrum which corresponds to these three peaks.

By the decomposition of water and hydrogen peroxide, OH,  $\text{HO}_2$ , and other oxygen radicals can be obtained. On analogy with these radicals, SH,  $\text{HS}_2$ , and  $(\text{S})_n$  are proposed. Gunning *et al.*<sup>8)</sup> obtained several spectra by the prolonged UV irradiation of pure  $\text{H}_2\text{S}$  and  $\text{H}_2\text{S}_2$  and their deuterides at the temperature of liquid nitrogen. They obtained very complex spectra; their identification was seemingly difficult. In their analysis, the spectrum of SH indicates a large  $g$  anisotropy and does not have an axial symmetry. As for hfs, Gunning *et al.* directly compared the gas-phase hfs with that of the solid phase; however, this is incorrect, as may be seen in Eqs. (1) and (2) of the Theoretical section.

From the electronic structure of the SH radical, the  $3p_x$  and  $3p_y$  orbitals of the sulfur atom, which are perpendicular to the molecular axis, are seen to be nearly degenerate. The principal  $g_{ii}$  values ( $i=x, y, z$ ) of the  $g$ -tensor can be written as;

$$g_{ii} = g_e - \sum_{n \neq p} 2\zeta | \langle p | L_i | n \rangle |^2 / (E_p - E_n) \quad (12)$$

where  $E$  is the energy of the unpaired electron orbital  $p$ , where  $E_n$  is that of the  $n$ th orbital, and where  $\zeta$  is the LS coupling constant. Assuming as the unpaired electron orbital the  $3p_x$  or  $3p_y$  orbital of a sulfur atom, and the SH bond as the  $n$ th orbital,  $g_{xx}$  and  $g_{yy}$  will give about the same value from Eq. (12) because of the near degeneracy. Eq. (12) indicates that an electronic structure like that of the SH radical will have an axial symmetric  $g$ -tensor. In our experiment, Fig. 4c shows almost axial symmetric spectra and a remarkable deuterium substitution effect; because they are radicals formed from a dilute solution of  $\text{H}_2\text{S}$  the radicals with more than two sulfur atoms may scarcely be formed. On the basis of these findings, this radical was identified with the SH radical. The superposed singlet spectrum of Fig. 4 showed no deuterium substitution effect. The trapped intermediate in the microwave discharge of sulfur vapor also gives a strong singlet line.<sup>24)</sup> Therefore, this line may be attributed to the  $(\text{S})_n$  radical.

This identification was also supported by the calculation. By the use of the  $g$ -tensor of the SD spectrum, which was determined by the spectrum simulation assuming that the hfs of deuterium was so small to neglect, the SH spectrum could be reproduced from the calculated hf tensor, *i.e.*,  $A_x = -3.5$ ,  $A_y = -3.5$ , and  $A_z = 0$  gauss. The simulated spectrum for SH is shown in Fig. 5 superposed on the observed spectrum.

In the case of the OH radical, the  $g$ - and hf-tensors were slightly different for each investigator. As for the SH radical, the influence of the trapped state may also change the spectral features; the discrepancy between the calculated and experimental results does not make the calculated results doubtful.

Recently Uehara and Morino<sup>25)</sup> observed rotation-

24) Unpublished result.

25) H. Uehara and Y. Morino, *J. Mol. Spectrosc.*, **36**, 158 (1970).

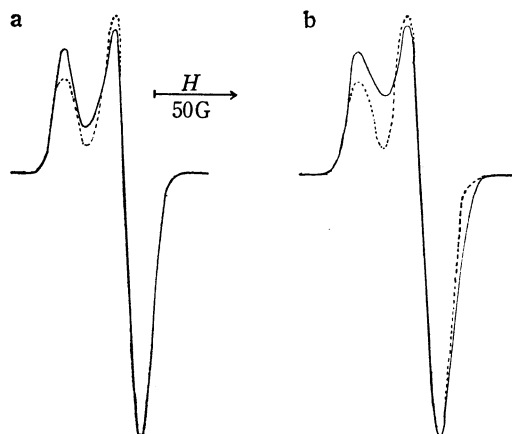


Fig. 5. Simulated spectra of SH ( $g_x=2.0023$ ,  $g_y=2.0100$ ,  $g_z=2.035$ ).

a, using hf-tensor from AHF orbital  
( $A_x=A_y=12.2$ ,  $A_z=0.5$  gauss)

b, using hf-tensor from the Slater orbital  
( $A_x=A_y=3.5$ ,  $A_z=0.0$  gauss)

broken line shows the observed spectra of SH.

ally-excited SH ( $J=5/2$ ) in the C-band. Though they could not resolve its hfs because of the large line-width, the accuracy of the calculation will be examined in the near future by gas-phase EPR or by microwave spectroscopy.

*Comparison of the Slater Orbital with the AHF Orbital on the Calculation of Anisotropic Terms.* In Fig. 6 the dependence of the values of  $\langle(3\cos^2\theta-1)/r^3\rangle_{av}$

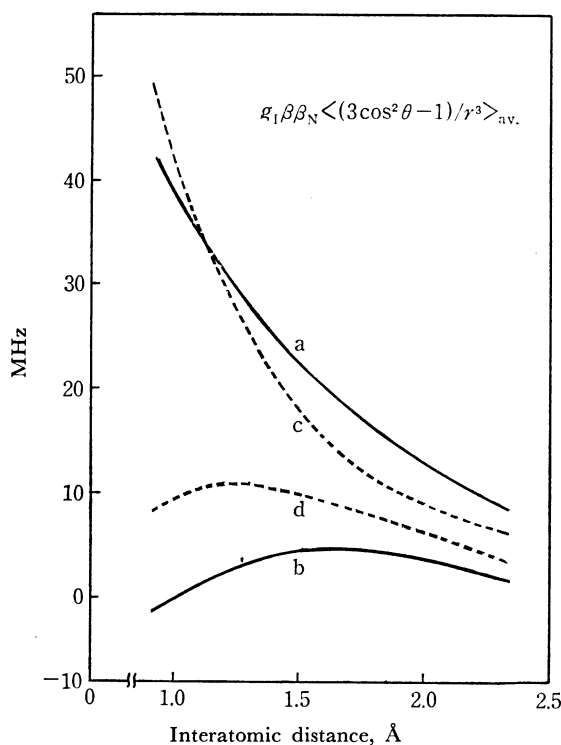


Fig. 6. Dependence of  $g_1\beta\beta_N\langle(3\cos^2\theta-1)/r^3\rangle_{av}$  on the interatomic distance.

a, AHF orbital of O

b, AHF orbital of S

broken line shows the value of the Slater orbital of O (c) and S (d).

on the interatomic distance between O and H and between S and H are shown for the Slater orbital and the AHF atomic orbital. The good agreement in the oxygen  $2p$  orbital shows that the shape of the oxygen  $2p$  Slater orbital fairly well resembles that of the AHF one. This may give support for the usefulness of the Slater orbital in MO calculation.

In SH, in spite of the large discrepancies from the AHF values, the value calculated using the Slater orbital as an unpaired electron orbital runs parallel with it. When we consider the nodeless property and the nonorthogonality of the Slater orbital, this parallelism is worth appreciating. Especially, the integrals calculated from  $3p$  orbital have a maximum value for both the Slater and AHF orbitals. This is characteristic not only of the  $3p$  orbital but also of the Slater  $4p$  orbital. The fact that the anisotropic dipolar interaction does not always decrease monotonously suggests that the hf interaction between indirectly-bonded atoms is sometimes important.

Figure 7 also shows the dependence of  $\langle(3\cos^2\theta-1)/r^3\rangle_{av}$  on the interatomic distance using the Slater orbitals of O, S, Se, and Te.

*SeH and TeH Radicals.* For the SeH radical, the unpaired electron orbital is assumed to be the  $4p$  Slater orbital or the AHF orbital, which consists of a linear combination of nine STO's of the selenium atom. For TeH, the  $5p$  Slater orbital of the tellurium atom is adopted. In this case, the assumption of the unpaired electron orbital as a pure  $p$  orbital is doubtful because, in the shell of the large-principal quantum number, the energy difference among the orbitals is

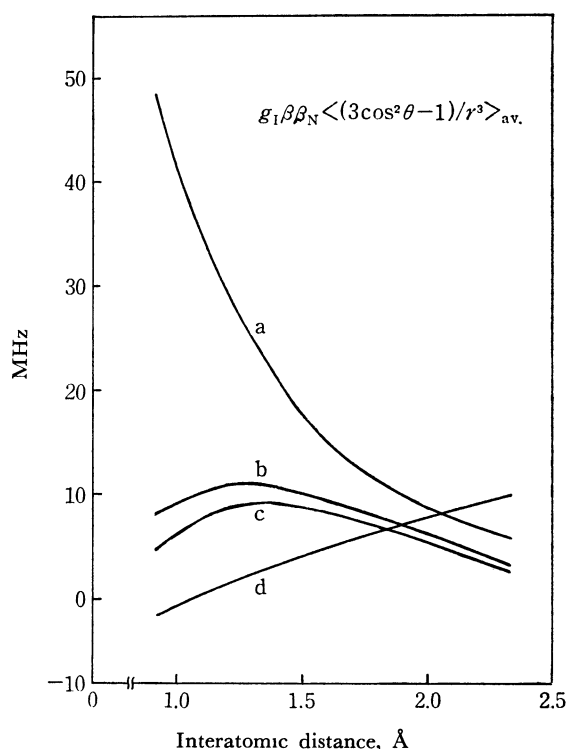


Fig. 7. Dependence of  $g_1\beta\beta_N\langle(3\cos^2\theta-1)/r^3\rangle_{av}$  of the Slater orbitals on the interatomic distance.

a, Oxygen b, Sulfur c, Selenium ( $n=3.5$ )

d, Selenium ( $n=4$ ) and Tellurium

small enough for them to be hybridized easily. The calculated anisotropic terms are somewhat large compared to those in OH and SH.

The trapped products formed by the reaction of the hydrogen atom with the evaporated films of metallic selenium and tellurium gave no EPR signal. Their metallic colors proved that the SeH and TeH radicals are primarily formed and then decomposed into metals and the hydrogen atom immediately after trapping. Because the products are trapped in a highly concentrated state, the hydrogen atom formed from the decomposition of SeH and TeH could not be detected.

By the UV photolysis of dilute aqueous solutions of  $\text{H}_2\text{Se}$  and  $\text{H}_2\text{Te}$  and their deuterides, the EPR signal of the hydrogen atom or the deuterium atom were

always detected. In this case, the SeH and the TeH radical are also unstable at the temperature of liquid nitrogen, and they decomposed into hydrogen atom and metals. The  $\text{H}_2\text{Se-H}_2\text{O}$  and the  $\text{H}_2\text{Te-H}_2\text{O}$  systems after the photolysis showed the color of red selenium and metallic tellurium. The hydrogen atom in this sample is less labile because of the surroundings, are mainly the water molecule, and the chance of the recombination is very small. The fact that the samples were always kept at the temperature of liquid nitrogen also stabilized the hydrogen atom. SeH and TeH are much unstable than OH and SH in both the gaseous and solid phases. Their stability is seemingly correlative with the strength of the reductivity of dihydrides.

---